

1 Combining accurate tumour genome simulation 2 with crowd-sourcing to benchmark somatic 3 structural variant detection

4
5 Anna Y. Lee^{1,12}, Adam D. Ewing^{2,3,12}, Kyle Ellrott^{2,4,12}, Yin Hu⁵, Kathleen E. Houlahan¹, J.
6 Christopher Bare⁵, Shadrielle Melijah G. Espiritu¹, Vincent Huang¹, Kristen Dang⁵, Zechen
7 Chong^{6,7,8}, Cristian Caloian¹, Takafumi N. Yamaguchi¹, ICGC-TCGA DREAM Somatic Mutation
8 Calling Challenge Participants, Michael R. Kellen⁵, Ken Chen⁶, Thea C. Norman⁵, Stephen H.
9 Friend⁵, Justin Guinney⁵, Gustavo Stolovitzky⁹, David Haussler², Adam A. Margolin^{4,5,13}, Joshua
10 M. Stuart^{2,13}, Paul C. Boutros^{1,10,11,13}

11
12 1 Ontario Institute for Cancer Research; Toronto, Ontario, Canada

13 2 Department of Biomolecular Engineering; University of California, Santa Cruz; Santa Cruz,
14 CA, USA

15 3 Mater Research Institute; University of Queensland; Woolloongabba, QLD, Australia

16 4 Computational Biology Program; Oregon Health & Science University; Portland, OR, USA

17 5 Sage Bionetworks; Seattle, WA, USA

18 6 Department of Bioinformatics and Computational Biology; University of Texas MD Anderson
19 Cancer Center; Houston, TX, USA

20 7 Department of Genetics; University of Alabama at Birmingham; Birmingham, AL, USA

21 8 Informatics Institute; University of Alabama at Birmingham; Birmingham, AL, USA

22 9 IBM Computational Biology Center; T.J.Watson Research Center; Yorktown Heights, NY,

23 USA

24 10 Department of Medical Biophysics; University of Toronto; Toronto, Ontario, Canada

25 11 Department of Pharmacology & Toxicology; University of Toronto; Toronto, Ontario, Canada

26 12 These authors contributed equally

27 13 Corresponding authors

28

29 Abstract

30 Background

31 The phenotypes of cancer cells are driven in part by somatic structural variants (SVs). SVs can
32 initiate tumours, enhance their aggressiveness and provide unique therapeutic opportunities.
33 Whole-genome sequencing of tumours can allow exhaustive identification of the specific SVs
34 present in an individual cancer, facilitating both clinical diagnostics and the discovery of novel
35 mutagenic mechanisms. A plethora of somatic SV detection algorithms have been created to
36 enable these discoveries, however there are no systematic benchmarks of them. Rigorous
37 performance evaluation of somatic SV detection methods has been challenged by the lack of
38 gold-standards, extensive resource requirements and difficulties in sharing personal genomic
39 information.

40 Results

41 To facilitate SV detection algorithm evaluations, we created a robust simulation framework for
42 somatic SVs by extending the BAMSurgeon algorithm. We then organized and enabled a
43 crowd-sourced benchmarking within the ICGC-TCGA DREAM Somatic Mutation Calling
44 Challenge (SMC-DNA). We report here the results of SV benchmarking on three different

45 tumours, comprising 204 submissions from 15 teams. In addition to ranking methods, we
46 identify characteristic error-profiles of individual algorithms and general trends across them.
47 Surprisingly, we find that ensembles of analysis pipelines do not always outperform the best
48 individual method, indicating a need for developing new ways to aggregate somatic SV
49 detection approaches.

50 **Conclusions**

51 The synthetic tumours and somatic SV detection leaderboards remain available as a community
52 benchmarking resource, and BAMSurgeon is available at
53 <https://github.com/adamewing/bamsurgeon>.

54 **Keywords**

55 somatic mutations, simulation, structural variants, benchmarking, cancer genomics, whole-
56 genome sequencing, crowd-sourcing

57

58 **Background**

59 Somatic structural variants (SVs) are mutations that arise in tumours involving rearrangements,
60 duplications or deletions of large segments of DNA. SVs are often defined to be events larger
61 than 100 bp in size, although with significant variability in this definition. Somatic SVs are critical
62 in driving and regulating tumour biology. They can initiate tumours [1,2] and because they are
63 unique to the cancer, can serve as highly-selective avenues for therapeutic intervention [3]. The
64 overall mutation load of somatic SVs serves as a proxy for genomic instability, and can robustly
65 predict tumour aggressiveness in multiple tumour types [4,5].

66 While somatic SVs that alter copy-number can be detected using microarray assays, the
67 resolution of such studies is limited, and many other important types of SVs cannot be detected.
68 As a result, high-throughput DNA sequencing is now a standard approach for detecting SVs in
69 cancer genomes. Although RNA-based assays are useful for detecting SVs that alter protein-
70 structure, DNA-based assays are required for most others. As a result, a broad range of
71 algorithms has been developed to detect SVs from short-read sequencing data using read
72 depth analysis, split read (*i.e.* a read that maps to different parts of the reference sequence)
73 alignment, paired end mapping and de novo assembly techniques [6–9]. However, the accuracy
74 of existing methods is poorly described. There are no comprehensive benchmarks of somatic
75 SV detection approaches. Most comparison results are reported by the developers of newly
76 published methods. These developer-run benchmarks are potentially subject to several types of
77 selection biases. For example, the developers of one tool may be experts in parameterizing and
78 tuning it, but may lack the same skill in tuning methods developed by others. Further, evaluating
79 the accuracy of somatic SV detection is more challenging than evaluating the accuracy of
80 somatic single nucleotide variant (SNV) detection as validation data is more difficult to generate
81 for SVs. Even the metrics of measuring accuracy are not agreed upon, with no community-
82 accepted standards on how SV prediction accuracy should be assessed, especially when
83 predictions are close to, but not exactly at, the actual sequence breakpoints. As a result, there
84 are no robust estimates of the false positive and false negative rates of somatic SV prediction
85 tools on tumours of different characteristics.

86 To fill this gap, we created an open challenge-based assessment of somatic SV prediction tools
87 as part of the ICGC-TCGA DREAM Somatic Mutation Calling Challenge (the Challenge). We
88 first extended BAMSurgeon [10], a tool for creating synthetic mutations, to generate somatic
89 SVs. We then created and distributed three synthetic tumours, on which 204 submissions were
90 made by 15 teams.

91 Results

92 Simulation of SVs with BAMSurgeon

93 In addition to point mutations [SNVs and short insertions or deletions (INDELs)], BAMSurgeon is
94 capable of creating SVs through read selection, local sequence assembly, manipulation of
95 assembled contigs, and simulation of sequence coverage over the altered contigs (Fig. 1a,
96 Additional file 1: Figure S1). This, combined with careful tracking of read depth, yields
97 approximations of SVs including insertions, deletions, duplication, and inversions into pre-
98 existing backgrounds of real sequence data. The BAMSurgeon manual, available online,
99 contains a full description of input formatting and available parameters. The input regions define
100 where local assembly will be attempted *via* Velvet [11]. For each region, the largest assembled
101 contig is selected and re-aligned to the reference genome using Exonerate [12]. The contig is
102 then trimmed to the length of its longest contiguous alignment and the alignment is used to
103 accurately track breakpoint locations within the contig in terms of reference coordinate space.
104 The location and identity of reads from the original BAM file in the assembled contig is tracked
105 *via* parsing of the AMOS [13] file output by Velvet [14], which also enables tracking of reads
106 included or excluded after contig trimming. If a suitable contig is not available for a given input
107 segment, no mutation is made for that segment. For each segment where contig assembly
108 succeeds, the contig is rearranged according to the user specification (*e.g.* insertion, deletion,
109 duplication, or inversion of sequence). Following rearrangement of the contig, paired reads are
110 simulated from the rearranged contig using wgsim [15], with specific parameters controllable by
111 the user. Because reads are simulated using the rearranged contig, breakpoint-spanning reads
112 and reads that will be discordant versus the reference genome assembly will be created. The
113 number of reads simulated (final coverage, C_f) depends on the original coverage C_o , the

114 difference in length between the original contig L_o and the rearranged contig L_f , and a user-
115 specified parameter controlling variant allele fraction (VAF). Thus, $C_f = VAF * C_o * (L_f / L_o)$.
116 Duplications and insertions result in larger contigs and require new reads to be added to the
117 final BAM, and deletions yielding a smaller contig require reads to be removed from the final
118 BAM. In cases where reads must be added (duplications and insertions), additional reads are
119 added to the final BAM. Conversely, where reads need to be removed from the original BAM, a
120 list of reads to be deleted is maintained, which correspond to reads covering the deleted region
121 in the original BAM.

122 **Validation of simulated somatic SVs**

123 To validate SVs simulated by BAMSurgeon, we performed a series of quality-control
124 experiments analogous to those performed to validate simulated SNVs [10]. Briefly, we used
125 BAMSurgeon to generate synthetic tumour-normal pairs, with the same set of target mutations,
126 that differ by the division of reads into tumour and normal sequence sets, aligner or cell line.
127 The target mutation set was designed to generate a synthetic tumour with a baseline level of
128 complexity and thus did not include insertions. We ran four SV callers using default parameters
129 on each pair: two widely used callers, CREST [16] and Delly [9], and two callers developed over
130 the course of the Challenge, Manta [17] and novoBreak [18]. We did not optimize parameters
131 for the callers since the goal of this validation was not to identify the best caller, but instead to
132 verify that the caller ranking is maintained across analogous datasets.

133 The definition of a SV suggests different scoring schemes for measuring the performance of a
134 caller. All SVs can be defined by at least one breakpoint; deletions, duplications and inversions
135 are SVs defined by a pair of breakpoints which in turn define a genomic region. Thus, we
136 compared called SVs to true-positive SVs based on i) region overlap or ii) breakpoint closeness
137 (Table 1, Additional file 1: Figure S2). The Challenge initially used a scoring scheme based on

138 region overlap (at least one or more bases in common; Additional file 1: Figure S2a). Here we
139 focus on the breakpoint closeness scheme since it is well suited for all types of SVs. A called
140 SV that is sufficiently similar to a known SV based on such criteria was considered a true
141 positive; otherwise, a false positive. We used such annotations to assess the performance of a
142 caller in terms of precision (fraction of calls that are true), recall (fraction of known SVs called)
143 and F -score (harmonic mean of precision and recall).

144 We performed several quality-control experiments. First, the caller ranking (by F -score) was
145 independent of the random division of reads: Manta > novoBreak > CREST > Delly (Additional
146 file 1: Figure S3a,b). Second, the same ranking was observed when alignments were generated
147 either using the Burrows-Wheeler Aligner (BWA) or NovoAlign with and without INDEL
148 realignment (*i.e.* local realignment to minimize mismatches across reads due to INDELS relative
149 to the reference genome), indicating that the ranking was independent of the aligner used (Fig.
150 1b, Additional file 1: Figure S3c). Lastly, when the genomic background was varied by using
151 HCC1143 BL or HCC1954 BL sequence data, the caller ranking was largely independent of the
152 cell line: Manta and novoBreak retained first and second place, respectively, while CREST and
153 Delly swapped places, although their F -scores were very similar to each other when HCC1954
154 BL was used (Fig. 1c, Additional file 1: Figure S3d). Overall, these results show that simulated
155 SVs are robust to changes in the read division, aligner and genomic background.

156 **Crowd-sourced benchmarking of somatic SV calling**

157 The SV component of the Challenge consisted of the same three synthetic tumour-normal data
158 sets used in the SNV component [10]. Briefly, the data sets were derived from existing cell line
159 sequence data (thus minimizing data access restrictions) and *in silico* tumours 1-3 (IS1-IS3)
160 were generated with increasing complexity (Fig. 1d). In terms of SVs, breakpoint locations were
161 randomly selected and the tumours had increasing mutation rates (371 vs. 2,886 somatic SVs in

162 IS1 and IS3, respectively). Moreover, IS1 contained deletions, duplications and inversions while
163 IS2 and IS3 additionally contained insertions. Like the SNV component, the SV component of
164 the Challenge was implemented using the Dialogue for Reverse Engineering Assessments and
165 Methods (DREAM) framework. Briefly, information about the Challenge was shared on its
166 website [19], participants registered online, downloaded a data set, applied their SV calling
167 pipelines to the data set and submitted the results in Variant Call Format (VCF) v4.1. IS1-IS3
168 were released sequentially, each data set had its own competition phase and participants could
169 make multiple submissions for each data set. Each tumour genome was divided into a training
170 set and a testing set by holding out a portion of the genome. During the competition phase,
171 leaderboards showed performance measures on the training set. After the competition closed,
172 leaderboards also showed performance measures on the whole genome (training + testing
173 sets).

174 The Challenge administration team prepopulated the leaderboards with two submissions and
175 the community provided 204 submissions from 15 teams (Additional file 2). A list of all
176 submissions, and descriptions of pipelines used to generate them, can be found in Additional
177 files 3 and 4, respectively. The submissions were surprisingly discordant in format. Some
178 specified SV types that are not recognized as VCF formatted types, and between 5.5-11% of all
179 submissions were not made in valid VCF format (Additional file 5). For this reason, and the
180 ambiguity of specifying SV types (*i.e.* the same SV can be specified with a specific type, or by
181 specifying the breakpoints and break-end adjacencies), type specifications were ignored when
182 scoring submissions. Team ranking varied with the stringency of the scoring (Additional file 1:
183 Figure S2d-i). For simplicity, we focused on scoring with $f = 100$ bp due to the balance between
184 the median and variance of the resulting F -scores (Additional file 1: Figure S4). While the top-
185 performing teams achieved near maximal precision on the simplest tumour, IS1, their recall
186 remained less than 0.9 (Fig. 2a), and decreased further on the other tumours (Additional file 1:

187 Figure S5a,b). On all three tumours, F -scores on the training and testing sets were highly
188 correlated (Spearman's rank correlation coefficient (ρ) ≥ 0.98 ; Fig. 2b, Additional file 1: Figure
189 S5c,d). However, the slightly elevated F -scores in the training sets observed for IS1 and IS2
190 may reflect minor overfitting; overfitting occurs when a statistical model is tuned to the training
191 set, limiting generalizability. Notably, the total number of somatic SV mutations in IS3 is $>4x$ that
192 for IS1 and IS2 (Fig. 1d). Conversely, the percentage of mutations used for training is greater for
193 IS1 (93%) and IS2 (92%) vs. IS3 (89%). Sampling from the IS3 mutations, we simulated training
194 and testing sets of different sizes, and computed the differences between the F -scores on the
195 training sets and the F -scores on the testing sets. We found that that the differences tend to be
196 greater when the percentage of mutations used for training is greater (Additional file 1: Figure
197 S5e). This suggests that the F -score differences observed for IS1 and IS2 are at least in part an
198 artefact of training set size.

199 Pipeline optimization

200 The within-team variability in F -scores accounts for 21-43% of the total per-tumour variance in
201 F -scores. The large variability in submissions by certain teams highlights the impact of tuning
202 parameters during the Challenge (Fig. 3a, Additional file 1: Figure S6a,b). In comparing the
203 initial ("naive") and best ("optimized") submissions of each team, for each tumour, the maximum
204 F -score improvement was 0.75 (from 0.12 to 0.87 by Team 5 for IS1), and the median
205 improvements were 0.20, 0.01, and 0.07 for IS1, IS2 and IS3, respectively (Fig. 3b). At least
206 33% of teams improved their F -score by at least 0.05 and at least 25% of teams improved it by
207 more than 0.20, depending on the tumour. Despite these improvements by parameterization,
208 team rankings were only moderately changed: if a team's naive submission ranked in the top
209 three, their optimized submission remained in the top three 66% of the time (Fig. 3c).

210 Given the crowd-sourced nature of the Challenge, we explored “wisdom of the crowds” as an
211 approach to optimize performance [20,21]. Specifically, we aggregated SV calls into an
212 ensemble by first identifying sufficiently similar calls in the majority of the top k submissions.
213 Pairwise distances between calls from different submissions were computed (*i.e.* a breakpoint-
214 length distance that incorporates distances between breakpoints and differences in SV length,
215 Additional file 1: Figure S2c), and those calls with distances less than a selected threshold
216 (equal to f , for consistency) were considered to represent an equivalent called SV event. The
217 chromosome together with the median start and end positions of a set of similar calls would
218 then define a single ensemble SV prediction. We considered two variations of this approach: i) a
219 baseline approach with ensembles of the best submission from each team, and ii) a
220 conservative approach with ensembles of all submissions and more stringent aggregation of
221 called SVs (see Methods). The baseline ensembles were found to have F -scores comparable to
222 that of the best submission (*e.g.* for IS1, the best ensemble and submission have F -scores of
223 0.92 and 0.91, respectively; Fig. 3d, Additional file 1: Figure S7b). However, the ensembles had
224 lower F -scores than the best submission for IS2 (Additional file 1: Figure S7a). When $k > 15$, we
225 found that the conservative ensemble F -scores drop further below that of the best submission
226 (Additional file 1: Figure S7c-e; *e.g.* for IS1, the best ensemble with $k > 15$ and the best
227 submission have F -scores of 0.83 and 0.91, respectively). In contrast, the precision of all
228 ensembles (range: 0.993-1.00) was similar or slightly improved compared to that of the best
229 submission. Thus, any changes in the ensemble F -scores were mostly influenced by the
230 changes in recall as k varied.

231 **Error characteristics**

232 We next exploited the large number of independent analyses to identify characteristics
233 associated with false negatives (FNs) and false positives (FPs). For example, error profiles

234 differed significantly between subclonal populations in IS3, with greater FN rates for mutations
235 present at lower VAFs (Additional file 1: Figure S8; one-sided Wilcoxon signed rank $P = 0.02$ for
236 $VAF = 0.2$ vs. 0.33 , $P = 0.04$ for $VAF = 0.33$ vs. 0.5 , $n = 7$). We also selected the best
237 submission from each team (by F -score) and focused on 14 variables associated with
238 breakpoint positions, representing factors like coverage and mapping quality (Additional file 6).
239 Several of these variables were associated with false-positive rates; in particular, tumour
240 coverage ($R > 0.24$), bridging reads count (the number of reads that bridge a putative
241 breakpoint, $R > 0.21$) and mapping quality ($R < -0.29$), have stronger associations with FPs for
242 both IS2 and IS3, compared to other variables (Additional file 1: Figure S9a, S10-S25). By
243 contrast, few were associated directly with false-negative rates ($0 \leq |R| \leq 0.15$; Additional file 1:
244 Figure S9b, S10-S25).

245 To evaluate whether these variables, and additional categorical variables, contribute
246 simultaneously to somatic SV prediction error, we generated two Random Forests (non-
247 parametric learning models that can trivially merge multiple data types) [22] for each team to
248 assess variable importance for FN and FP breakpoints separately. FN breakpoints are
249 associated with variables such as high bridging reads count and strand bias (Fig. 4a,c,e,g,i;
250 Additional file 1: Figure S26a). FP breakpoints are generally associated with variables such as
251 low mapping quality (Fig. 4b,d,f,h,j; Additional file 1: Figure S26b).

252 By executing specific SV callers, CREST (Fig. 4a,b), Delly (Fig. 4c,d) and Manta (Fig. 4e,f), with
253 the same parameters on all three tumours, we identified tumour-specific error profiles. For
254 example, the distance to the nearest germline INDEL tends to have stronger associations with
255 errors in IS2 and IS3 compared to IS1 (Fig. 4a-e). Team-specific error profiles are more
256 apparent with the FP breakpoint analysis. For example, Teams 8 and 10 have distinct FP
257 profiles for the same tumour, IS2 (Fig. 4h); FPs by Teams 8 and 10 are negatively and positively

258 associated with tumour coverage, respectively. Algorithmic approaches to SV calling from
259 sequencing data include i) read depth analysis, ii) paired end mapping, iii) split read alignment,
260 and iv) *de novo* assembly [23]. Some teams submitted sufficient algorithm details to determine
261 the general approaches used, as well as the choice of aligner (Fig. 4g-j). Based on the available
262 annotations, teams using the same aligner do not have error profiles that tightly cluster for all
263 three tumours, suggesting that the aligner is not as strong a driver of those profiles, compared
264 to the caller algorithm.

265

266 Discussion

267 Crowd-sourced benchmarking challenges are ideal for questions where significant diversity in
268 algorithmic approaches exists, particularly where individual methods are highly parameterized
269 or computationally intensive [24,25]. The detection of variants from high-throughput sequencing
270 data fits these criteria well: dozens of algorithms are in common use, many with complicated
271 sets of parameters to tune and most requiring tens to hundreds of CPU hours to execute. We
272 have quantified the critical importance of parameterization: it accounts for 21-43% of the
273 variability in performance across the 204 submissions evaluated. This is comparable to the 26%
274 of variability observed in somatic SNV detection benchmarking [10], and highlights the need for
275 algorithm developers to continue to optimize parameters, provide guidance for their tuning and
276 work toward automating their selection to make their software easier to use.

277 The “wisdom of the crowds” is the idea that an ensemble of multiple algorithms can significantly
278 outperform any individual method. Several crowd-sourced benchmarking competitions from
279 diverse fields have shown great success in combining submissions from contestants to achieve
280 a high-performing meta-predictor including challenges for somatic SNV detection [10], gene

281 regulatory network inference [21] and mRNA-based prognostic signatures for breast cancer
282 [20]. By contrast, in somatic SV detection, we do not have clear evidence that an ensemble
283 improves on the best individual method consistently across different tumours, despite testing
284 several ways of creating ensembles. This may reflect the large diversity in the biases of each
285 individual algorithm (Fig. 4), or it may represent the unique challenges of scoring SVs. While
286 some SV classes may be well-represented by overlap-based scoring methods, others benefit
287 more from breakpoint-based scoring, and the choice of scoring metric and parameter must be
288 tuned to the specific biological question of interest. For example, breakpoint identification is
289 critical when considering translocations -- especially those generating candidate fusion proteins
290 -- while overlap of the called and known regions is much more important for copy-number
291 analyses. The fact that the “wisdom of the crowds” *via* majority vote approach works very well
292 for somatic SNV detection, it appears to fail for somatic SV detection. Thus there is a need for
293 continued development of new, more complex ways to integrate multiple somatic SV detection
294 methods [26].

295 Given the paucity of gold-standard benchmarking data for somatic SVs, the creation of the
296 simulated datasets and the associated leaderboards constitutes a major contribution of this
297 Challenge. There are distinct advantages to benchmarking on simulated datasets. It is
298 dramatically easier to simulate large numbers of tumours, or to create tumours with highly
299 divergent mutational properties, leading to well-supported estimates of per-tumour caller
300 accuracy. This enables our strategy of generating synthetic tumours of increasing complexity by
301 facilitating assessment of the impact of the complexity introduced at each step. Specifically, it is
302 possible to identify strengths and weaknesses of an individual caller by comparing its tumour-
303 specific error profiles. Moreover, synthetic tumours can be designed to test the limits of callers.
304 These advantages highlight the usefulness of synthetic datasets for benchmarking callers, and
305 until synthetic datasets are completely realistic, they will serve as important complements to real

306 datasets. While 15 teams participated in the actual competitive phase of the Challenge, 8 teams
307 have exploited the IS1-3 benchmarking resources since the competition, making 73
308 submissions to benchmark their methods for pipeline evaluation and development. We hope
309 that journals will begin to expect benchmarking on these standard datasets, as well as those
310 being generated by the final phases of the ICGC-TCGA DREAM Somatic Mutation Calling
311 Challenge, as a standard part of manuscripts reporting new somatic SV detection algorithms.

312

313 Conclusions

314 Analysis of the error profiles of the Challenge submissions showed that somatic SV calling is a
315 distinctly harder problem than somatic SNV calling, with individual pipelines having complex and
316 unique error profiles. Parameterization was a critical factor in determining the performance of
317 teams. Finally, we demonstrate that, unlike almost every past DREAM Challenge, somatic SV
318 prediction does *not* benefit from the “wisdom of the crowds” -- simple voting of multiple
319 prediction pipelines does not yield improved predictions in this instance. The synthetic tumours
320 and somatic SV detection leaderboards remain available as a community benchmarking
321 resource.

322

323 Methods

324 Simulation of SVs by BAMSurgeon

325 SV support in BAMSurgeon has evolved throughout the Challenge, largely as a result of
326 constructive feedback from participants. Our descriptions of BAMSurgeon's method for
327 simulating SVs is current as of commit (*i.e.*, version) b851573474 of the code available at [27].

328 As input, BAMSurgeon (addsv.py) requires an indexed reference genome, a pre-existing BAM
329 file (Additional file 1: Figure S1a), and a list of intervals (Additional file 1: Figure S1b) along with
330 the SV type and parameters (see manual [28]). The intervals should be wide enough that local
331 sequence assembly is successful in generating a contig that spans at least 2x the expected
332 library size in the input BAM file. Intervals for which a sufficiently long contig cannot be
333 generated are rejected, where the exact definition of 'sufficiently long' is an optional parameter.
334 Intervals which contain too many discordant read pairs are also rejected, subject to a
335 parameter. Following local assembly, the contig is re-arranged: the specific rearrangements for
336 each supported SV type are illustrated in Fig. 1a (step iii) and Additional file 1: Figure S1c,e,g.
337 The assembled contig is then re-aligned to the target interval in the reference genome
338 (exonerate --bestn 1 -m ungapped) and is trimmed based on the start and end coordinates of
339 this alignment. Read pairs corresponding to trimmed contig sequence are removed from further
340 consideration.

341 Read coverage is generated over the rearranged contig using a read simulator (wgsim -e 0 -R 0
342 -r 0), to achieve the same average depth as the input BAM file, which has the effect of creating
343 split reads relative to the reference genome supporting SV detection. For a deletion, the number
344 of reads required to achieve (e.g.) 30x coverage is fewer than the number of reads required to
345 reach 30x coverage prior to the deletion, so reads must be removed from the original BAM (Fig.
346 1a, step iv). Inversely, for duplications and insertions additional reads need to be added to the
347 original BAM (Additional file 1: Figure S1d,h). Inversions generally do not affect coverage
348 (Additional file 1: Figure S1f). To ensure any reads removed actually correspond to the deleted
349 region of the contig, the locations of reads in the assembled contig are tracked. The number of
350 reads to be replaced, added, or deleted is scaled with the desired allele fraction. Finally, any
351 read pairs in the original BAM corresponding to reads altered in the simulated SV are replaced,
352 any read pairs marked for deletion are removed from the original BAM, and any additional read

353 pairs generated are added. It is recommended that the resulting altered BAM be post-processed
354 (with `postprocess.py`) to ensure compliance with the SAM format specification (see manual
355 [28]).

356 **Synthetic tumour generation**

357 Synthetic tumours were prepared by partitioning high-coverage BAMs from 'normal' cell lines
358 into two groups of reads, picking read pairs at random as described previously [10]. For the
359 three *in silico* challenges, non-overlapping regions were selected at random for SV addition,
360 resulting in 371 variants added for IS1, 655 for IS2, and 2,886 for IS3 (Fig. 1d). Variant input
361 files are available in Additional file 7. SVs were added using `addsv.py` with assembly
362 GRCh37/hg19 as the reference genome and default parameters except where noted. For IS3,
363 to simulate subclones a file specifying CNV fractions over SV regions was input via option `-c` to
364 specify the variant allele frequency (VAF) of the spiked-in variants at either 0.5, 0.33, or 0.2
365 (Additional file 7). The output BAMs were post-processed to account for any inconsistencies
366 introduced due to remapping and merging of reads supporting SVs using the script
367 `postprocess.py` included with `BAMSurgeon`. The BAMs were further adjusted with
368 `RealignerTargetCreator` and `IndelRealigner` from the Genome Analysis Toolkit (v.2.4.9). All
369 tumour-normal pairs generated via `BAMSurgeon` are verified for adherence to the SAM/BAM
370 format specification using the `ValidateSamFile` tool included in the Picard tool set [29]. Truth
371 VCF files, *i.e.* files specifying simulated mutations, for SVs were generated using the script
372 `etc/makevcf_sv.py` and merged with truth files for SNP and INDEL locations, where applicable.
373 `SAMtools` was used throughout to split, merge, sort, and index BAMs, and also index FASTA
374 files. Details on the specific `BAMSurgeon` commits used for generating each tumour, as well as
375 other tumour details are given at [30].

376 **Validation of BAMSurgeon**

377 To validate BAMSurgeon's ability to simulate somatic SVs, we compared the output of four
378 algorithms -- two widely used SV callers, CREST [16] and Delly [9], and two callers developed
379 over the course of the Challenge, Manta [17] and novoBreak [18] -- on the IS1 tumour-normal
380 data set, and analogous datasets generated with the same spike-in set of mutations, but with an
381 alternate aligner (NovoAlign v.3.00.05 [31]), cell line (HCC1954 BL) or read division. We did not
382 optimize parameters for the callers since the goal of this validation was not to identify the best
383 caller, but instead to verify that the caller ranking is maintained across analogous datasets.

384 Each tumour-normal pair was processed by CREST (v1.0) to extract soft clipping positions for
385 each chromosome separately, using default parameters. This data was then used by CREST to
386 call somatic SVs using the default protocol, and we converted the output into VCF v4.1 format.
387 Somatic SVs were called from each tumour-normal pair using Delly (v0.5.5) with default
388 parameters. Calling was performed on each chromosome separately for all supported SV types
389 except for translocations, and we converted the translocation output into VCFv4.1 format. Calls
390 with MAPQ < 20, PE < 5, or labeled as "LowQual" or "IMPRECISE" were filtered out. Somatic
391 SVs were called from each tumour-normal pair using Manta (v0.26.3) with the following
392 parameters: -m local -j 4 -g 10. Lastly, somatics SVs were called from each dataset using
393 novoBreak (v1.04) with a modification to ensure that sequence windows around breakpoints
394 never go beyond the start of the chromosome. All sets of SV calls were scored with $f = 100$ bp
395 and $j > 0$, callers were ranked based on F -score for each tumour-normal pair, and rankings were
396 compared across pairs (Fig. 1b,c and Additional file 1: Figure S3).

397 **Preprocessing VCF files**

398 We preprocess VCF files to parse out the SV-relevant details (e.g. the END coordinate in the
399 INFO value or from the length of the REF sequence; if the END coordinate cannot be

400 determined from those values, it is set to the POS coordinate), remove SVs that did not pass
401 filters (as indicated by the FILTER values) and ensure consistent formatting between files. To
402 ensure consistent formatting in accordance with the VCFv4.1 specification [32] we:

- 403 1. Add row entries to ensure that each MATEID specification has a corresponding pair of
404 entries, where only a single entry is provided
- 405 2. Re-assign IDs and MATEIDs to ensure unambiguous references to entries
- 406 3. Where possible, replace SVTYPE = BND entries with entries specifying SVTYPE =
407 {CNV, DEL, DUP, INS, INV} in accordance with REF, ALT and EVENT values

408 Testing set SVs are indicated in the truth VCF file with the addition of masked genomic regions
409 specified with CHROM, POS and END values indicating the chromosome, start and end
410 coordinates, and SVTYPE = MSK. Specifically, a SV where $\geq 50\%$ of the corresponding region
411 overlaps a masked region is allocated to the testing set; otherwise, it is in the training set.

412 **Structural variant scoring**

413 Our scoring approaches evaluate the accuracy of a set of called SVs and requires input VCF
414 files specifying: i) called SVs, and ii) true/known SVs. Generally, a called SV that is sufficiently
415 similar to a known SV based on specific criteria (Table 1) is considered a true positive (TP);
416 otherwise, a false positive (FP). Also, a known SV that is sufficiently similar to a called SV is
417 considered a TP; otherwise, a false negative (FN). Our scoring supports two ways of quantifying
418 similarity:

419 A. **Region overlap.** The Jaccard coefficient (j) is computed from the lengths (in bp) of
420 intersection and union regions (Additional file 1: Figure S2a).

421 **B. Breakpoint closeness.** The distance (Δ , in bp) between called and known breakpoints
422 is computed (Additional file 1: Figure S2b). If $\Delta \leq f$ (where f is a flank threshold
423 parameter), a relative closeness is computed, $c' = 1 - \Delta/f$. The overall closeness (c) is
424 defined as the geometric mean of the c' values for the start and end breakpoints. If only
425 one of the start and end breakpoints has $\Delta \leq f$, the called and known SVs are annotated
426 as partially matching.

427 Unless otherwise specified, we scored with $f = 100$ bp. If there is an ambiguous matching of
428 called SVs to known SVs by sufficient similarity, the similarity values (j/c) are used to identify an
429 optimal one-to-one matching. First, we restrict the matching to the best match(es) for each
430 called and known SV. If a SV has multiple best matches by similarity, we attempt to break the
431 tie by favouring SVs with the same SVTYPE, and/or test/training set membership. If the best
432 matching is still ambiguous, we then use corresponding similarity values together with the
433 Hungarian algorithm to obtain a one-to-one matching (with the `clue` v0.3-48 R package [33]).
434 Finally, SVs are annotated based on this matching. SVs that have sufficient similarity but are not
435 in the final matching are annotated as partially matching. Mated breakpoints are initially
436 annotated separately. If one is annotated as partially matching or as a TP, and the other is a FP,
437 the FP annotation is replaced by a partial match annotation. Subsequently, each set of mated
438 breakpoints is treated as a single SV.

439 These annotations are used to assess the performance of a SV caller in terms of precision =
440 $nTP/(nTP + nFP)$, recall = $nTP/(nTP + nFN)$ and F -score (specifically, F_1 -score) = $2 \times \text{precision} \times$
441 $\text{recall}/(\text{precision} + \text{recall})$, where nTP , nFP and nFN represent the numbers of TPs, FPs and
442 FNs, respectively. Partial matches are not counted in these computations. Unless otherwise
443 specified, the precision, recall and F -score values presented here were computed on the testing

444 and training sets combined. The best submission of a given team is defined as the team's
445 submission with the greatest F -score computed against all known SVs.

446 **Execution of challenge-based benchmarking**

447 The SV component of the Challenge was executed concurrently with the SNV component, and
448 the procedure has been described previously [10]. It was implemented using the Dialogue for
449 Reverse Engineering Assessments and Methods (DREAM) framework. Briefly, information
450 about the Challenge was shared on its website [19], participants registered online, downloaded
451 a data set, applied their SV calling pipelines to the data set and submitted the results in
452 VCFv4.1 format. IS1-IS3 were released sequentially, each data set had its own competition
453 phase and participants could make multiple submissions for each data set. Each tumour
454 genome was divided into a training set and a testing set. During the competition phase,
455 leaderboards showed performance measures on the training set. After the competition closed,
456 leaderboards also showed performance measures on the whole genome (training + testing
457 sets), thus benchmarking the SV calling pipelines. The SV leaderboards for IS1 and IS2 were
458 pre-populated with results from BreakDancer (v1.1.2_2013_03_08 [7]) run with default
459 parameters; a reference point submission indicated labeled as "Standard" in figures and tables.
460 Due to our exploration of multiple SV scoring methods in this manuscript, the leaderboard
461 results are not completely consistent with the results presented here, but all raw and
462 leaderboard data are available.

463 **Overfitting artefact analysis**

464 Due to the order of magnitude greater number of SVs spiked into IS3, we simulated training and
465 testing sets of different sizes by sampling from the IS3 training set. Specifically, we assessed
466 mutation totals of 100 to 1000 (by increments of 100), and training sets that were 80-95% (by
467 increments of 1%) of the total, by sampling each {mutation-total, training-set%} combination 100

468 times. For each sample, we computed $F_{train} - F_{test}$ for each IS3 submission where F_{train} and F_{test}
469 are F -scores computed on the simulated training and testing sets, respectively. We then
470 computed the median difference across samples to obtain a summary value for each
471 submission, and finally show the median across submissions in Additional file 1: Figure S5e.
472 ($F_{train} - F_{test}$) > 0 suggests overfitting but such values are an artefact of testing set size since no
473 fitting/training was done in this analysis.

474 **Team variation**

475 For each tumour-normal pair, we computed the percentage of variation in F -score, across all
476 submissions, that is accounted for by within-team variation. Specifically, we computed the
477 within-team sum of squares as a percentage of the total sum of squares.

478 **Definition of ensembles**

479 We aggregated SV calls from k submissions into an ensemble set with the following general
480 approach:

- 481 1. **BND filter.** Calls defined with SVTYPE = BND were excluded for simplicity.
- 482 2. **Compute call distances.** Pairwise distances (d , in bp) between remaining predictions
483 were computed (*i.e.* a breakpoint-length distance that incorporates distances between
484 breakpoints and differences in predicted SV length, Additional file 1: Figure S2c).
485 Distances were only computed between predictions from different submissions.
- 486 3. **Generate sets of similar calls.** A distance less than a selected threshold (100 for
487 consistency with f , see **Structural variant scoring**) indicated sufficiently similar calls.

488 We assessed two variations:

- 489 a. **Baseline.** We defined a graph such that vertices represented calls and edges
490 connected sufficiently similar calls. We identified the connected components to

491 define the sets of similar calls. Sets with median intra-set distances $> f$ were
492 refined. Specifically, the call with the greatest median distance to the other set
493 members was iteratively removed until the median intra-set distance dropped
494 below f , or the set became empty.

495 b. **Conservative.** We used the added constraint that called SVs overlap by ≥ 1 bp
496 to be treated as sufficiently similar. Sets of similar calls were constructed by
497 iterating over the sufficient similarity pairs from least to most distant. If a pair did
498 not contain a call in an existing call set, the pair was used to define a new call
499 set. Otherwise, one call was already in a set, and the other was a candidate for
500 addition to the same set via guilt-by-association. If the candidate came from a
501 submission that was not already covered by the set, and its median distance to
502 the existing set members $\leq f$, it was added to the set. Any unprocessed pairs
503 within or between the prediction sets at that stage were excluded from
504 consideration.

505 4. **Majority vote filter.** Sets with calls from $\leq k/2$ submissions were excluded; each
506 remaining set covered the majority of submissions.

507 5. **Aggregate sets to define ensemble calls.** The chromosome together with the median
508 start and end positions of each set of calls defined a single ensemble SV call.

509 An additional distinction between the baseline and conservative approaches is that the baseline
510 approach only involved the best submission from each team whereas all submissions were

511 used with the conservative approach. To investigate different ensembles of N submissions for
512 the same tumour-normal pair, we first ordered the submissions by overall F -score, computed
513 after excluding calls with SVTYPE = BND. We then generated an ensemble call set with the top
514 k submissions, for $k = 2..N$. The performance of ensembles was compared to that of the
515 individual submissions, after excluding calls with SVTYPE = BND (e.g. Fig. 3d).

516 **Error characterization**

517 To characterize the errors made by a team, we assessed the team's best submission for a given
518 tumour-normal pair. We also assessed errors made by CREST, Delly and Manta when run, with
519 the same protocols described in the **Validation of BAMSurgeon** section, on all three tumour-
520 normal pairs. Characterizing FNs and FPs involved comparisons to TPs and true negatives
521 (TNs), respectively. Moreover, we characterized errors at the level of breakpoints.

522 **Sampling true negatives.** Given a set of submissions for the same tumour-normal pair, we
523 identified the maximum number of FPs from a single submission, m . We then sampled $\geq m$ TNs
524 for each submission, by sampling regions from the reference genome that satisfied these
525 criteria:

- 526 1. length sampled from a log-normal distribution with mean and standard deviation equal to
527 that of the logged lengths of the known SVs
- 528 2. start position is not in known gap and repeat regions
- 529 3. region does not overlap with any known SVs
- 530 4. region does not overlap with any SVs called in the submission

531 Some sampled regions qualified as TNs for multiple submissions. For IS2, we excluded Team
532 14's submission because it had a very large number (17,806) of FPs, and thus was
533 computationally problematic for the subsequent Random Forest analysis.

534 **Breakpoint annotations based on scoring.** A single breakpoint may be associated with
535 multiple (called/known) SVs, and therefore may be associated with multiple annotations
536 depending on the scoring approach used, *i.e.* > 1 of {TP, FN, FP}. To remove ambiguity, we
537 choose a single annotation for each breakpoint by prioritizing as follows: TP > FN > FP. This
538 prioritization favours good performance (*i.e.* TP has highest priority) and then recall (*i.e.* FN >
539 FP) since it appears to be a greater challenge than precision for SV calling (Fig. 2a, Additional
540 file 1: Figure S5a,b). TN breakpoints should be unambiguous due to the way in which they were
541 sampled (see above).

542 **Genomic variables.** For each breakpoint position, we computed 16 genomic factors, 12 of
543 which were previously described [10]. The additional genomic variables were computed as
544 follows:

- 545 A. **Bridging reads count.** We used samtools v0.1.19 to identify reads in the tumour BAM
546 mapped to a genomic region containing the window defined by the breakpoint position
547 +/- 1 bp. The bridging read count was defined as the number of identified reads. Note
548 that a bridging read does not necessarily have a secondary mapping for part of the read,
549 as one might expect for a split read.
- 550 B. **Distance to nearest germline INDEL.** Germline calls were obtained as previously
551 described [10] and INDELS were parsed out. The distance of a breakpoint to the nearest
552 germline INDEL was computed using BEDTools closest v2.18.2.
- 553 C. **Nucleotide complexity.** The sequence for the window defined by the breakpoint
554 position +/- 50 bp was extracted from the reference fasta file. The nucleotide complexity
555 was defined as the entropy of the sequence: $-\sum p_x \log_2(p_x)$ over $x \in \{A, G, C, T\}$ where p_x
556 is the proportion of the sequence with x (case-insensitive).

557 D. **Strand bias.** We used samtools v0.1.19 to identify reads in the tumour BAM mapped to
558 a genomic region containing the breakpoint position. The strand bias was defined as the
559 proportion of these reads mapped to the + strand.

560 **Univariate analysis.** To assess the relationship between each non-categorical variable and
561 prediction error rates, we computed the Pearson correlation coefficient between the variable
562 values and the proportion of teams with a FN/FP at the breakpoints, as well as the
563 corresponding *P* value. Reference and alternative allele counts, base quality, tumour and
564 normal coverages, bridging reads counts and distances to the germline SNP and INDEL were
565 logged (base 10) prior to computing correlations (zeros were replaced with -1 instead of
566 logged). For the categorical variables, trinucleotide and genomic location, the *P* value measured
567 the significance of the variable in a fitted binomial model predicting the FN/FP rate at a
568 breakpoint. A binomial model was fitted because it is a relatively simple model (and thus less
569 prone to overfitting) to test the relationship between a categorical variable and a proportion
570 variable (*i.e.* an error rate).

571 **Multivariate analysis.** Random Forests were generated as previously described [10] with a few
572 alterations. Here, a total of 16 genomic variables (Fig. 4) were used to build: i) a classifier to
573 distinguish FN and TP breakpoints, and ii) a classifier to distinguish FP and TN breakpoints. A
574 FP classifier was not generated for Team 7 with respect to IS1 since the team produced only
575 one FP, and thus there was insufficient data to generate an accurate model. Conversely, a FP
576 classifier was not generated for Team 14 with respect to IS2 since the team produced a very
577 large number of FPs (17,806) that caused a failure to converge. Computation of the directional
578 effect of variables was also as previously described [10].

579 Non-parametric tests (*i.e.* Wilcoxon and Mann-Whitney tests) were used throughout to avoid
580 assumptions about the distributions of the tested populations; all tested populations had $n \geq 7$.

581 The BEDTools suite (v2.18.2 [34]) was used with the bedR R package (v0.5.3 [35]) throughout.
582 Plots were generated with the BPG (v5.3.9), lattice (v0.20-33) and latticeExtra (v0.6-26) R
583 packages and R (v3.2.1) was used throughout.

584

585 **Declarations**

586 **Availability of data and materials**

587 Sequences files are available at the Sequence Read Archive (SRA) under accession number
588 SRP042948. BAMSurgeon [commit (*i.e.*, version) b851573474] is available at [27]. Submission
589 and known mutation (*i.e.* ground truth) VCF files are available from the Challenge website [19]
590 following registration and subsequent login.

591 **Acknowledgments**

592 The authors thank S.P. Shah, R.D. Morin and P.T. Spellman for helpful suggestions, L.E.
593 Heisler and B.F. Huang as well as all the members of the Boutros lab for insightful discussions
594 and technical support. The authors thank Google Inc. (in particular N. Deflaux) and Annai
595 Biosystems (in particular D. Maltbie and F. De La Vega) for their ongoing support of the ICGC-
596 TCGA DREAM Somatic Mutation Calling Challenge.

597 The ICGC-TCGA DREAM Somatic Mutation Calling Challenge Participants are: Bret D. Barnes,
598 Inanc Birol, Xiaoyu Chen, Readman Chiu, Anthony J. Cox, Li Ding, Markus H-Y. Fritz, Andrey
599 Grigoriev, Faraz Hach, Joseph K. Kawash, Jan O. Korbel, Semyon Kruglyak, Yang Liao,
600 Andrew McPherson, Ka M. Nip, Tobias Rausch, S. Cenk Sahinalp, Iman Sarrafi, Christopher T.
601 Saunders, Ole Schulz-Trieglaff, Richard Shaw, Wei Shi, Sean D. Smith, Lei Song, Difei Wang,
602 Kai Ye.

603 **Funding**

604 This study was conducted with the support of the Ontario Institute for Cancer Research to
605 P.C.B. through funding provided by the Government of Ontario. This work was supported by
606 Prostate Cancer Canada and is proudly funded by the Movember Foundation - Grant #RS2014-
607 01. This study was conducted with the support of Movember funds through Prostate Cancer
608 Canada and with the additional support of the Ontario Institute for Cancer Research, funded by
609 the Government of Ontario. This project was supported by Genome Canada through a Large-
610 Scale Applied Project contract to P.C.B., S.P. Shah and R.D. Morin. This work was supported
611 by the Discovery Frontiers: Advancing Big Data Science in Genomics Research program, which
612 is jointly funded by the Natural Sciences and Engineering Research Council (NSERC) of
613 Canada, the Canadian Institutes of Health Research (CIHR), Genome Canada, and the Canada
614 Foundation for Innovation (CFI). P.C.B. was supported by a Terry Fox Research Institute New
615 Investigator Award and a CIHR New Investigator Award. K.E.H. was supported by a CIHR
616 Computational Biology Undergraduate Summer Student Health Research Award. A.D.E was
617 supported by an Australian Research Council Discovery Early Career Researcher Award
618 DE150101117 and by the Mater Foundation. The following National Institutes of Health (NIH)
619 grants supported this work: R01-CA180778 (J.M.S.), and U24-CA143858 (J.M.S.). The funders
620 played no role in study design, data collection, data analysis, data interpretation or in writing of
621 this manuscript.

622 **Author's contributions**

623 A.A.M., J.M.S and P.C.B. initiated the project. A.D.E. created BAMSurgeon. A.D.E, K.E., Y.H.,
624 K.E.H., J.C.B., M.R.K., T.C.N., S.H.F., G.S., A.A.M., J.M.S. and P.C.B. created the ICGC-TCGA
625 DREAM Somatic Mutation Calling Challenge. A.Y.L., A.D.E., Y.H., K.E.H., S.M.G.E., V.H., K.D.,
626 Z.C., C.C., and T.N.Y. created datasets and analyzed sequencing data. A.Y.L., Y.H., K.E.H, and

627 P.C.B. were responsible for statistical modelling. Research was supervised by K.C., S.H.F.,
628 J.G., G.S., D.H., A.A.M., J.M.S. and P.C.B. The first draft of the manuscript was written by
629 A.Y.L. and P.C.B., extensively edited by A.D.E., K.E., A.A.M. and J.M.S. and approved by all
630 authors.

631 **Ethics approval and consent to participate**

632 Not applicable.

633 **Consent for publication**

634 Not applicable.

635 **Competing interests**

636 All authors declare that they have no competing interests.

637 **Additional files**

638 Additional file 1: Figures S1-S26. (PDF)

639 Additional file 2: Table S1. Challenge participation. (XLS)

640 Additional file 3: Table S2. All competition-phase submissions evaluated with $f = 100$ and $j > 0$.
641 (XLS)

642 Additional file 4: Descriptions of pipelines used to generate submissions. (PDF)

643 Additional file 5: Table S3. Invalid SV types. (XLS)

644 Additional file 6: Table S4. Univariate error analysis. (XLS)

645 Additional file 7: BAMSurgeon input files used to generate the three *in silico* tumour-normal
646 pairs (IS1-IS3). (TAR.GZ)

647

648 **Table 1 | Caller scoring schemes.**

Basis of comparison	Region Overlap (Additional file 1: Figure S2a)	Breakpoint Closeness (Additional file 1: Figure S2b)
Description	SVs match if there is sufficient overlap, determined with a Jaccard threshold parameter, between the genomic region associated with the called SV and that of the known SV	SVs match if the breakpoints of the called SV are sufficiently close to the those of the known SV, <i>i.e.</i> breakpoints are within f bp of one another where f is a flank parameter
Strengths	<ul style="list-style-type: none"> • identifies genomic regions affected by the known SVs 	<ul style="list-style-type: none"> • suited to all types of SVs • evaluates precision of breakpoint predictions, facilitating subsequent breakpoint validation
Weaknesses	<ul style="list-style-type: none"> • some SVs are not accurately defined by genomic regions, e.g. an insertion may be characterized by a single breakpoint • need criteria to define sufficient overlap 	<ul style="list-style-type: none"> • need criteria to define sufficient closeness

649

650

651 Figure Legends

652 **Fig. 1 | BAMSurgeon simulates SVs in genome sequences.**

653 Method for adding SVs to existing BAM alignments. **a** Overview of SV (e.g. deletion) spike-in:
654 Starting with an original BAM (i), a region (ii) is selected where a deletion is desired. iii) Contigs
655 are assembled from reads in the selected region, and the contig is rearranged by deleting the
656 middle. The amount of contig deleted is a user-definable parameter. Read coverage is
657 generated over the contig using wgsim to match the number of reads per base in the original
658 BAM. Since the deletion contig is shorter than the original, fewer reads will be required to
659 achieve the equivalent coverage. iv) Generated read pairs include discordant pairs (*i.e.* paired
660 reads that do not align to the reference genome with the expected relative orientation and inner
661 distance) spanning the deletion and clipped reads (*i.e.* reads that are only partially aligned to the
662 reference). Reads mapping to the deleted region of the contig are not included in the final BAM.
663 **b,c** To test the robustness of BAMSurgeon with respect to changes in **(b)** aligner and **(c)** cell
664 line, we compared the ranks of CREST, Delly, Manta and novoBreak on two new tumour-normal
665 data sets: one with an alternative aligner, NovoAlign, and the other on an alternative cell line,
666 HCC1954 BL. Callers were scored with $f = 100$ bp (Additional file 1: Figure S2b); Manta retained
667 the top position, independent of aligner and cell line. **d** Summary of the three *in silico* (IS)
668 tumours described here. Abbreviations: DEL, deletion; DUP, duplication; INV, inversion; INS,
669 insertion.

670 **Fig. 2 | Overview of the SV Calling Challenge submissions.**

671 **a** Precision-recall plot of IS1 submissions. Each point represents a submission, each colour
672 represent a team and the best submission from each team (top F -score) is circled. The
673 “Standard” point corresponds to the reference point submission provided by Challenge

674 organizers. **b** The F -scores of submissions on the training and testing sets are highly correlated
675 for IS1 (Spearman's $\rho = 0.98$), falling near the plotted $y = x$ line.

676 **Fig. 3 | Performance optimization by parameterization and ensembles.**

677 **a** Recall, precision and F -score of all IS1 submissions plotted by team, then submission order.
678 Teams were ranked by the F -score of their best submission, colour coding (top bar) as in Fig. 2.
679 The “Standard” lines correspond to the reference point submission provided by Challenge
680 organizers. **b** For each tumour, the improvement in F -score from the initial (“naive”) to the best
681 (“optimized”) submissions of each team. Darker shades of blue indicate greater improvement. **c**
682 For each tumour, team rankings based on their naive or optimized submissions. Larger dot
683 sizes indicate better ranks by F -score. **b,c** An “X” indicates that the team did not make a
684 submission for the specific tumour (or changed team name). **d** Recall, precision and F -score of
685 ensembles versus individual submissions for IS1. At the k th rank, the triangles indicate
686 performance of the ensemble of the top k submissions, and the circles indicate performance of
687 the k th ranked submission. The ensemble analysis focused on the best submission from each
688 team.

689 **Fig. 4 | Characteristics of prediction errors.**

690 Random Forests assess the importance of 16 sequence-based variables for each caller's FN
691 (**a,c,e,g,i**) and FP (**b,d,f,h,j**) breakpoints. Each panel shows variable importance on the left,
692 where each row represents the best performing set of predictions by the given team/caller (on
693 the given *in silico* tumour), and each column represents the indicated variable. Dot size reflects
694 variable importance, *i.e.* the mean change in accuracy caused by removing the variable from
695 the model (generated to predict erroneous breakpoints). Colour reflects the directional effect of
696 each variable (red and blue for greater and lower variable values, respectively, associated with
697 erroneous breakpoints; black for categorical variables or insignificant directional associations,

698 two-sided Mann-Whitney $P > 0.01$). Background shading indicates the accuracy of the model
699 (see colour bar). Variable importance for FN and FP breakpoints in each of the three tumours is
700 shown for the following SV callers: CREST (**a,b**), Delly (**c,d**) and Manta (**e,f**). Manta only called
701 two FPs in IS1; thus, variable importance for FP breakpoints could not be computed (indicated
702 by Xs in the plot). Variable importance for FN and FP breakpoints in IS2 (**g,h**) and IS3 (**i,j**) is
703 shown for each team. In the right plot (**g-j**), the first four columns indicate usage of the indicated
704 algorithmic approaches by each team, and the last column indicates the aligner used. Grey
705 indicates that algorithmic approaches and aligner are unknown for the given team.
706 Abbreviations: Algm, algorithm; SNP, single-nucleotide polymorphism; INDEL, short insertion or
707 deletion.

708

709 References

- 710 1. Northcott PA, Lee C, Zichner T, Stütz AM, Erkek S, Kawauchi D, et al. Enhancer
711 hijacking activates GFI1 family oncogenes in medulloblastoma. *Nature*. 2014;511:428–
712 34.
- 713 2. Taub R, Kirsch I, Morton C, Lenoir G, Swan D, Tronick S, et al. Translocation of the c-
714 myc gene into the immunoglobulin heavy chain locus in human Burkitt lymphoma and
715 murine plasmacytoma cells. *Proc. Natl. Acad. Sci. U. S. A.* 1982;79:7837–41.
- 716 3. Huang M, Ye Y, Chen S, Chai J, Lu J, Zhao L, et al. Use of all-trans retinoic acid in the
717 treatment of acute promyelocytic leukemia. *Blood*. 1988;72.
- 718 4. Lalonde E, Ishkanian AS, Sykes J, Fraser M, Ross-Adams H, Erho N, et al. Tumour
719 genomic and microenvironmental heterogeneity for integrated prediction of 5-year
720 biochemical recurrence of prostate cancer: a retrospective cohort study. *Lancet. Oncol.*
721 2014;15:1521–32.

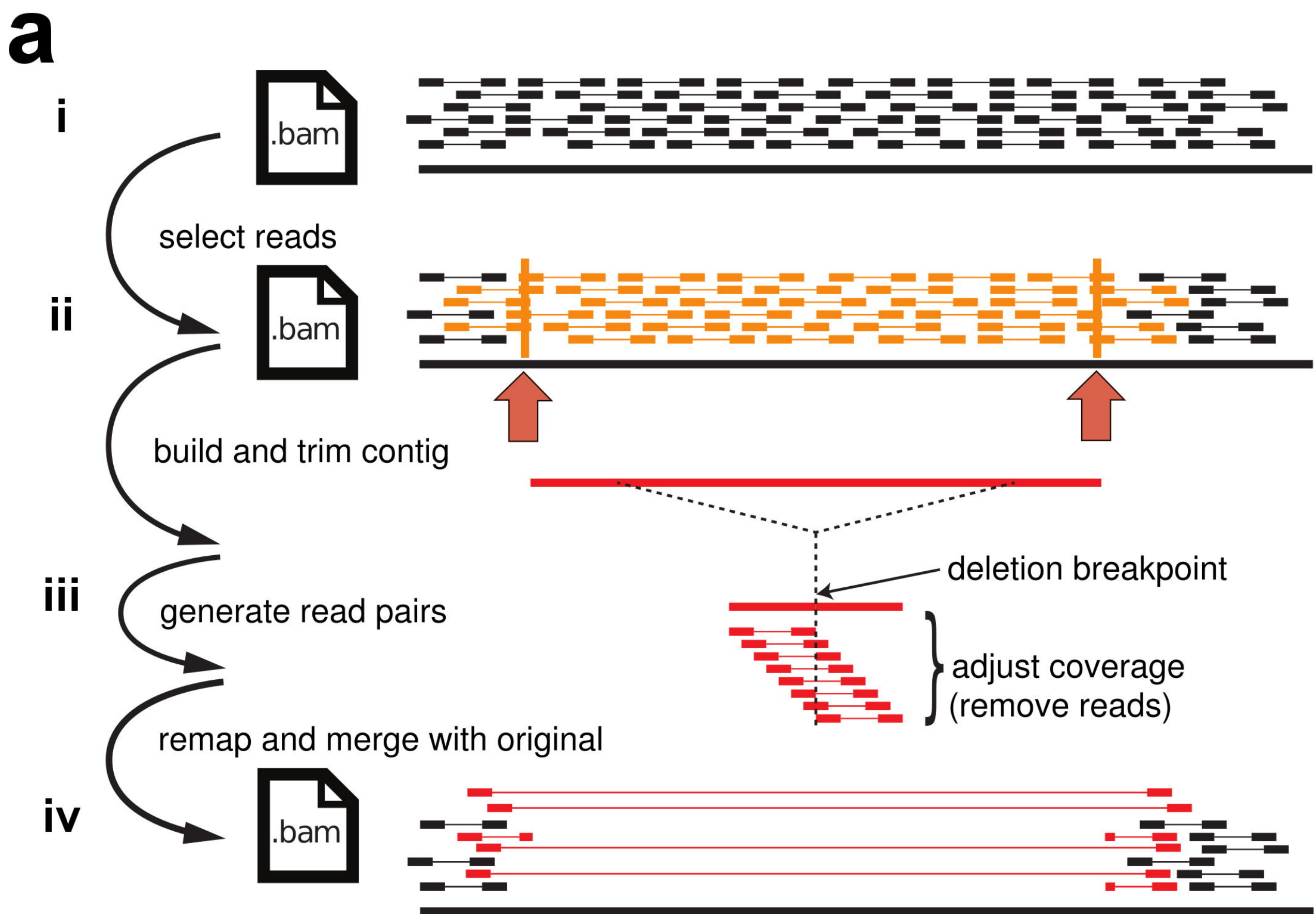
- 722 5. Vollan HKM, Rueda OM, Chin S-F, Curtis C, Turashvili G, Shah S, et al. A tumor DNA
723 complex aberration index is an independent predictor of survival in breast and ovarian
724 cancer. *Mol. Oncol.* 2015;9:115–27.
- 725 6. Medvedev P, Stanciu M, Brudno M. Computational methods for discovering structural
726 variation with next-generation sequencing. *Nat. Methods.* 2009;6:S13–20.
- 727 7. Chen K, Wallis JW, McLellan MD, Larson DE, Kalicki JM, Pohl CS, et al. BreakDancer:
728 an algorithm for high-resolution mapping of genomic structural variation. *Nat. Methods.*
729 2009;6:677–81.
- 730 8. Hormozdiari F, Hajirasouliha I, Dao P, Hach F, Yorukoglu D, Alkan C, et al. Next-
731 generation VariationHunter: combinatorial algorithms for transposon insertion discovery.
732 *Bioinformatics.* 2010;26:i350-7.
- 733 9. Rausch T, Zichner T, Schlattl A, Stütz AM, Benes V, Korbel JO. DELLY: structural variant
734 discovery by integrated paired-end and split-read analysis. *Bioinformatics.* 2012;28:i333–
735 9.
- 736 10. Ewing AD, Houlahan KE, Hu Y, Ellrott K, Caloian C, Yamaguchi TN, et al. Combining
737 tumor genome simulation with crowdsourcing to benchmark somatic single-nucleotide-
738 variant detection. *Nat. Methods.* 2015;12:623–30.
- 739 11. Zerbino DR, Birney E. Velvet: algorithms for de novo short read assembly using de Bruijn
740 graphs. *Genome Res.* 2008;18:821–9.
- 741 12. Slater GSC, Birney E. Automated generation of heuristics for biological sequence
742 comparison. *BMC Bioinformatics.* 2005;6:31.
- 743 13. Pop M, Phillippy A, Delcher AL, Salzberg SL. Comparative genome assembly. *Brief.*
744 *Bioinform.* 2004;5:237–48.
- 745 14. Zerbino DR, McEwen GK, Margulies EH, Birney E. Pebble and rock band: heuristic
746 resolution of repeats and scaffolding in the velvet short-read de novo assembler.

- 747 Salzberg SL, editor. PLoS One. 2009;4:e8407.
- 748 15. GitHub Code Repository: wgsim. <https://github.com/lh3/wgsim>. Accessed 22 November
749 2017.
- 750 16. Wang J, Mullighan CG, Easton J, Roberts S, Heatley SL, Ma J, et al. CREST maps
751 somatic structural variation in cancer genomes with base-pair resolution. *Nat. Methods*.
752 2011;8:652–4.
- 753 17. Chen X, Schulz-Trieglaff O, Shaw R, Barnes B, Schlesinger F, Källberg M, et al. Manta:
754 rapid detection of structural variants and indels for germline and cancer sequencing
755 applications. *Bioinformatics*. 2016;32:1220–2.
- 756 18. Chong Z, Ruan J, Gao M, Zhou W, Chen T, Fan X, et al. novoBreak: local assembly for
757 breakpoint detection in cancer genomes. *Nat. Methods*. 2017;14:65–7.
- 758 19. ICGC-TCGA DREAM Mutation Calling challenge.
759 <https://www.synapse.org/#!Synapse:syn312572/wiki/58893>. Accessed 22 November
760 2017.
- 761 20. Margolin AA, Bilal E, Huang E, Norman TC, Ottestad L, Mecham BH, et al. Systematic
762 analysis of challenge-driven improvements in molecular prognostic models for breast
763 cancer. *Sci. Transl. Med*. 2013;5:181re1.
- 764 21. Marbach D, Costello JC, Küffner R, Vega NM, Prill RJ, Camacho DM, et al. Wisdom of
765 crowds for robust gene network inference. *Nat. Methods*. 2012;9:796–804.
- 766 22. Strobl C, Boulesteix A-L, Zeileis A, Hothorn T. Bias in random forest variable importance
767 measures: illustrations, sources and a solution. *BMC Bioinformatics*. 2007;8:25.
- 768 23. Tattini L, D’Aurizio R, Magi A. Detection of Genomic Structural Variants from Next-
769 Generation Sequencing Data. *Front. Bioeng. Biotechnol*. 2015;3:92.
- 770 24. Boutros PC, Margolin AA, Stuart JM, Califano A, Stolovitzky G. Toward better
771 benchmarking: challenge-based methods assessment in cancer genomics. *Genome Biol*.

- 772 2014;15:462.
- 773 25. Meyer P, Alexopoulos LG, Bonk T, Califano A, Cho CR, de la Fuente A, et al. Verification
774 of systems biology research in the age of collaborative competition. *Nat. Biotechnol.*
775 2011;29:811–5.
- 776 26. Mohiyuddin M, Mu JC, Li J, Bani Asadi N, Gerstein MB, Abyzov A, et al. MetaSV: an
777 accurate and integrative structural-variant caller for next generation sequencing.
778 *Bioinformatics.* 2015;31:2741–4.
- 779 27. GitHub Code Repository: BAMSurgeon. <https://github.com/adamewing/bamsurgeon>.
780 Accessed 22 November 2017.
- 781 28. BAMSurgeon Manual.
782 <https://github.com/adamewing/bamsurgeon/blob/master/doc/Manual.pdf>. Accessed 22
783 November 2017.
- 784 29. Picard Tools - By Broad Institute. <http://broadinstitute.github.io/picard/>. Accessed 22
785 November 2017.
- 786 30. ICGC-TCGA DREAM Mutation Calling challenge: Synthetic Tumours.
787 <https://www.synapse.org/#!Synapse:syn312572/wiki/62018>. Accessed 22 November
788 2017.
- 789 31. Novocraft. <http://www.novocraft.com/>. Accessed 22 November 2017.
- 790 32. The Variant Call Format (VCF) Version 4.1 Specification. [https://samtools.github.io/hts-
791 specs/VCFv4.1.pdf](https://samtools.github.io/hts-specs/VCFv4.1.pdf). Accessed 22 November 2017.
- 792 33. Kuhn HW. The Hungarian method for the assignment problem. *Nav. Res. Logist. Q.*
793 Wiley Subscription Services, Inc., A Wiley Company; 1955;2:83–97.
- 794 34. Quinlan AR, Hall IM. BEDTools: a flexible suite of utilities for comparing genomic
795 features. *Bioinformatics.* 2010;26:841–2.
- 796 35. Haider S, Waggott D, Lalonde E, Fung C, Liu F-F, Boutros PC. A bedr way of genomic

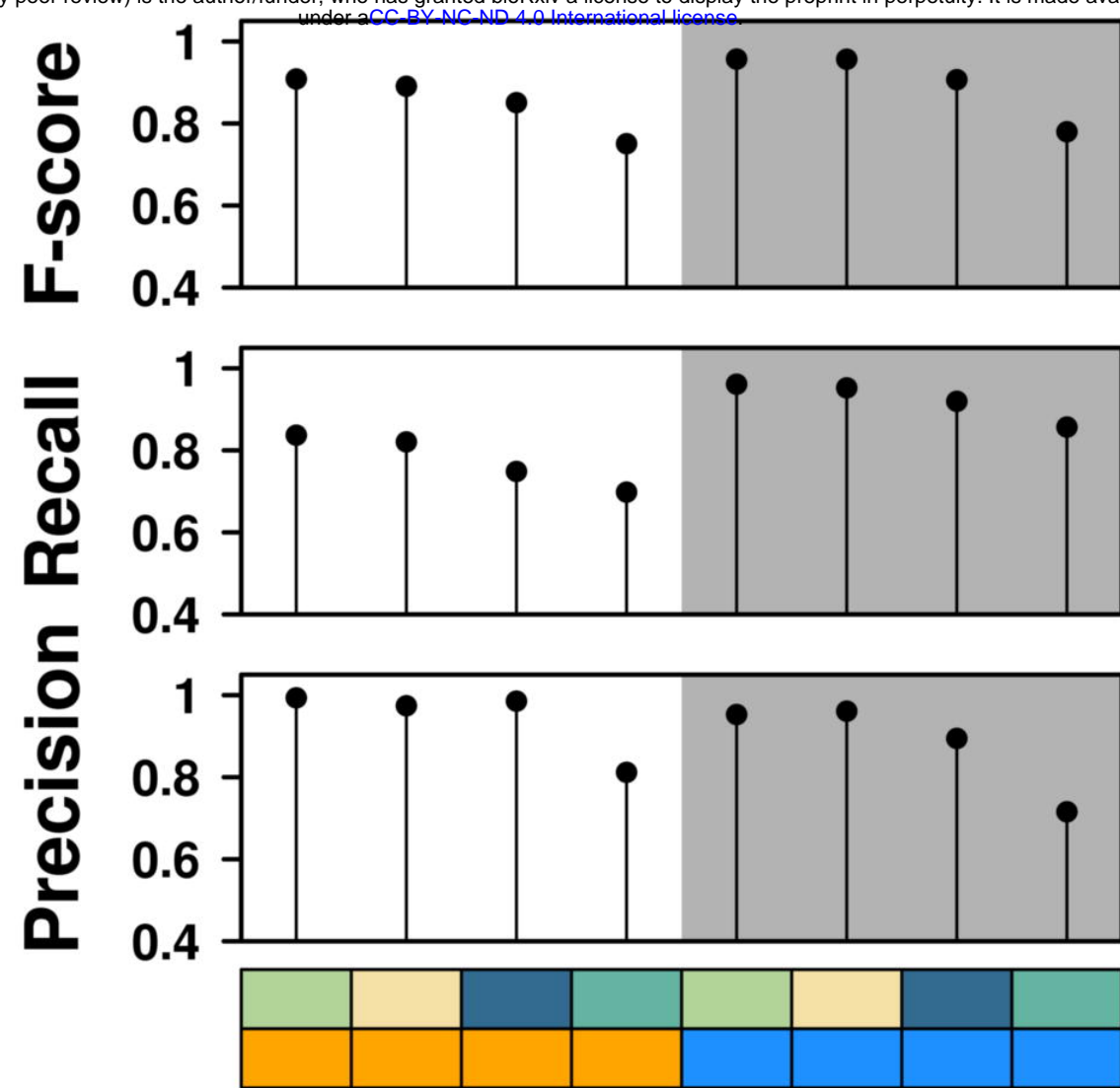
797 interval processing. Source Code Biol. Med. 2016;11:14.

798

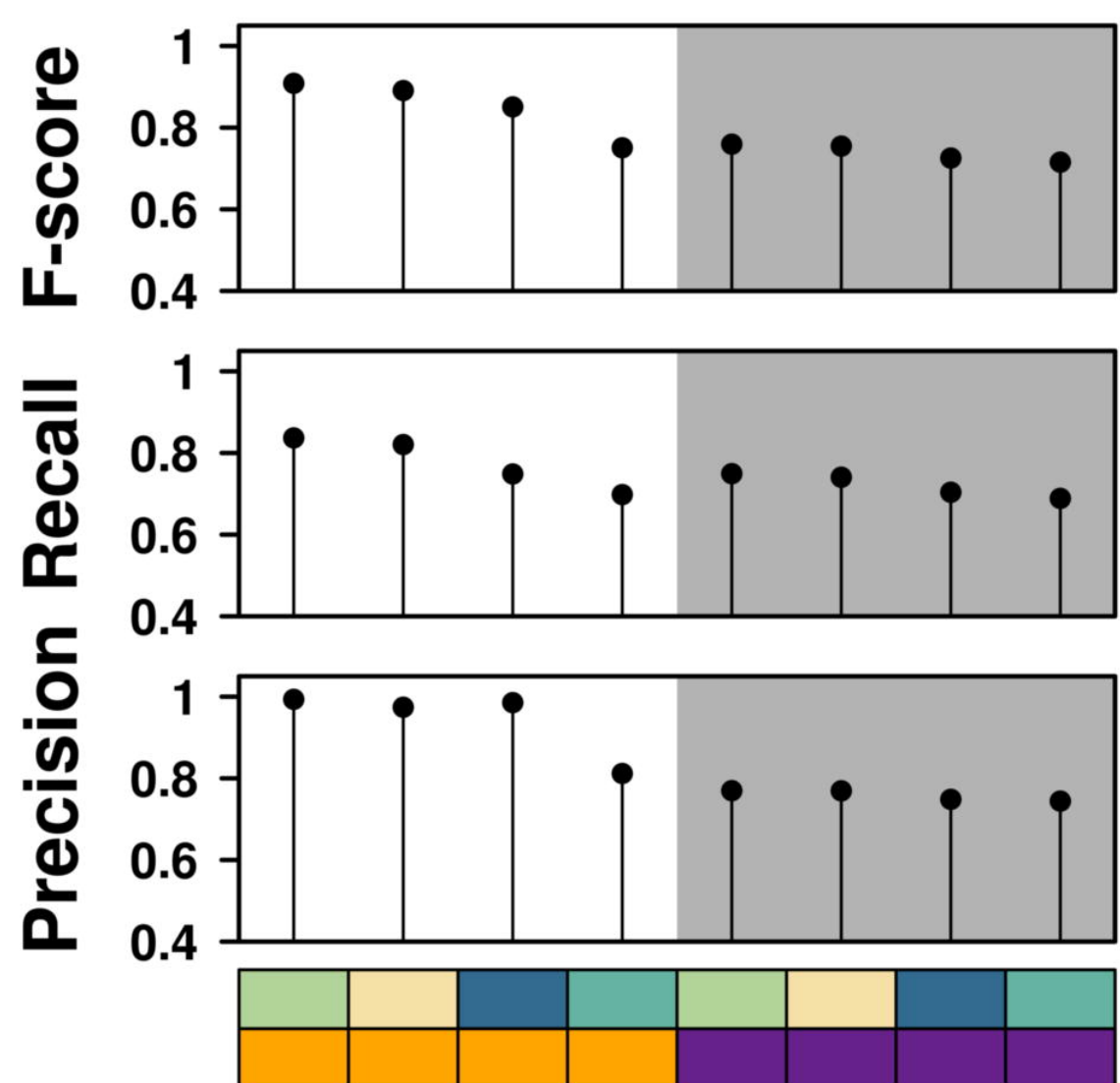


b

bioRxiv preprint doi: <https://doi.org/10.1101/224733>; this version posted November 25, 2017. The copyright holder for this preprint (which was not certified by peer review) is the author/funder, who has granted bioRxiv a license to display the preprint in perpetuity. It is made available under aCC-BY-NC-ND 4.0 International license.

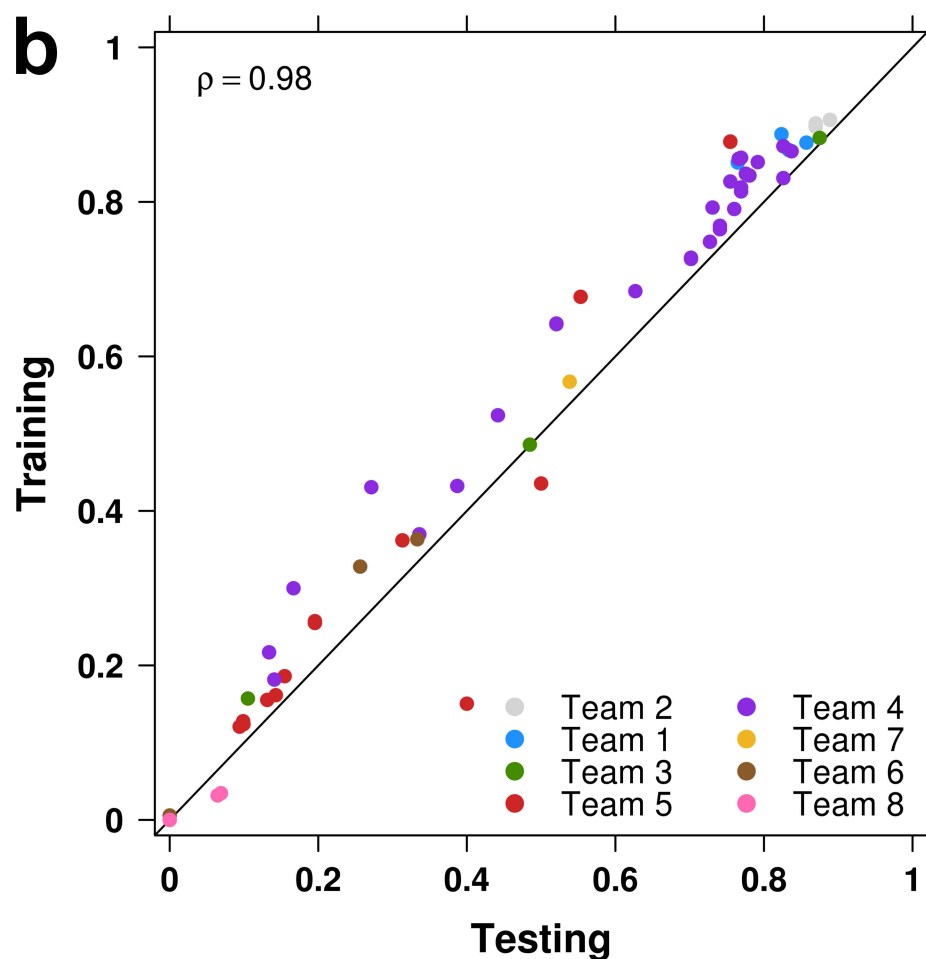
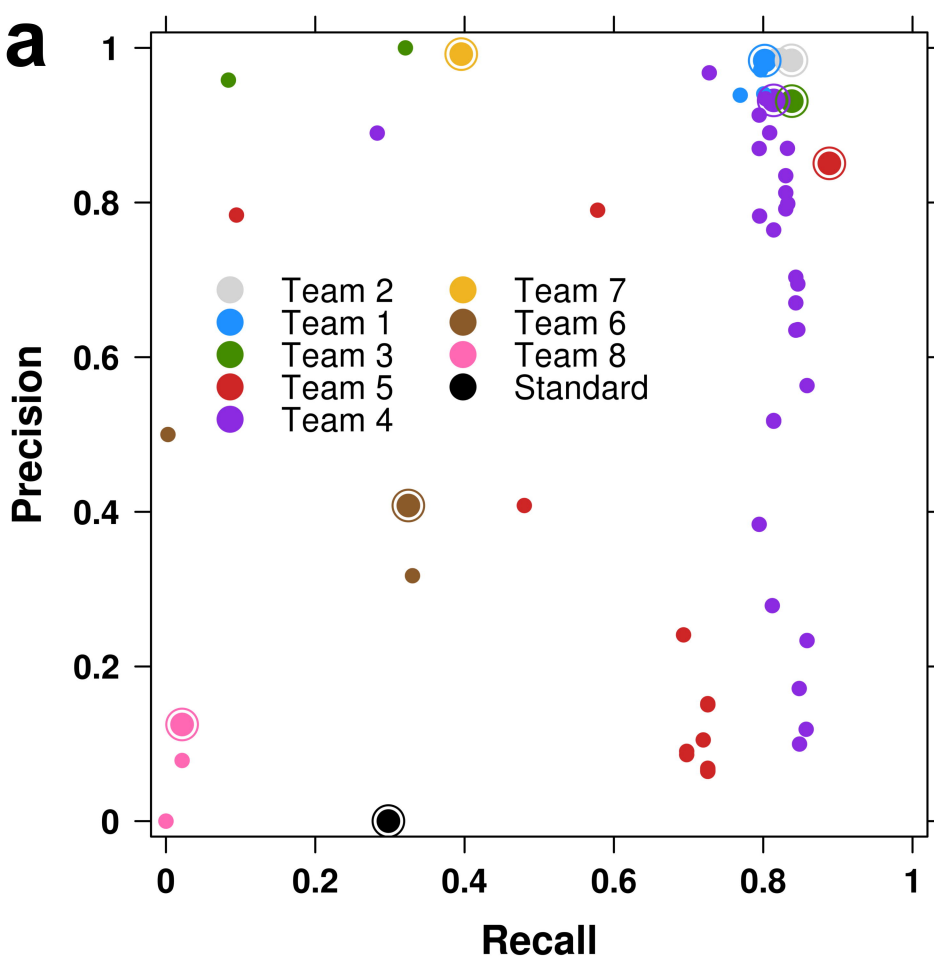


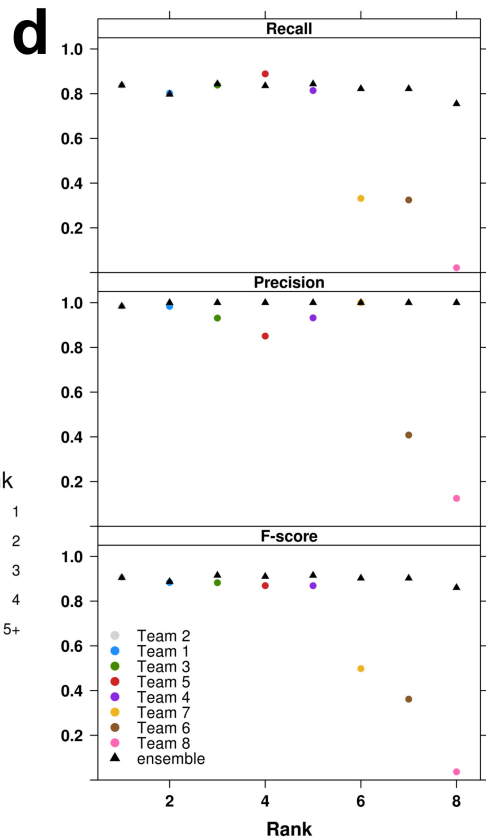
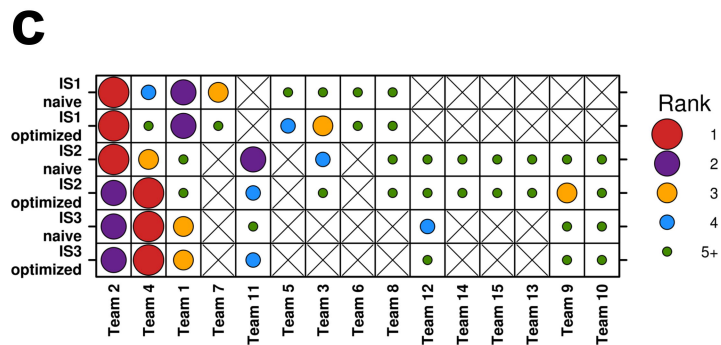
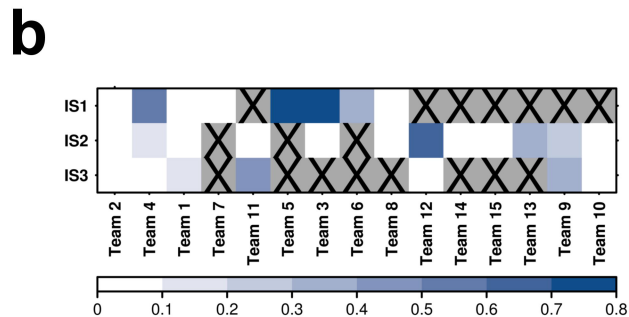
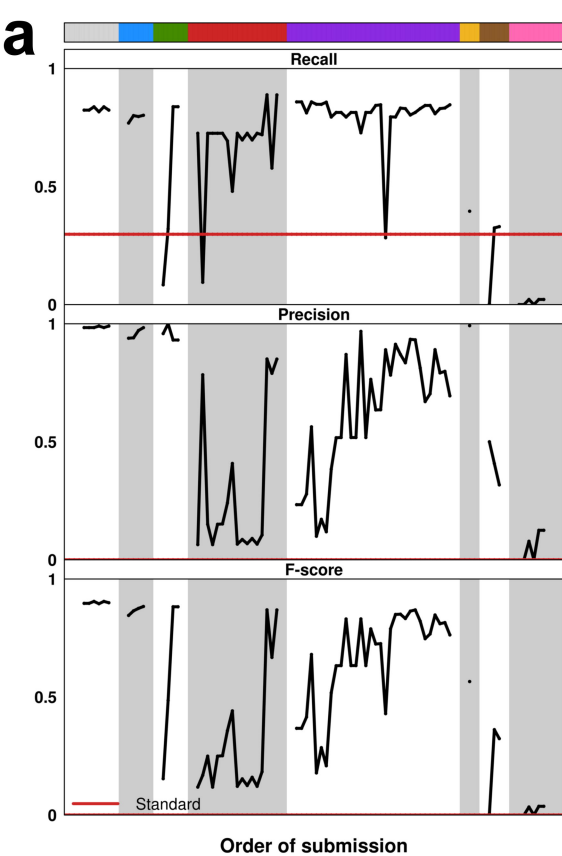
c



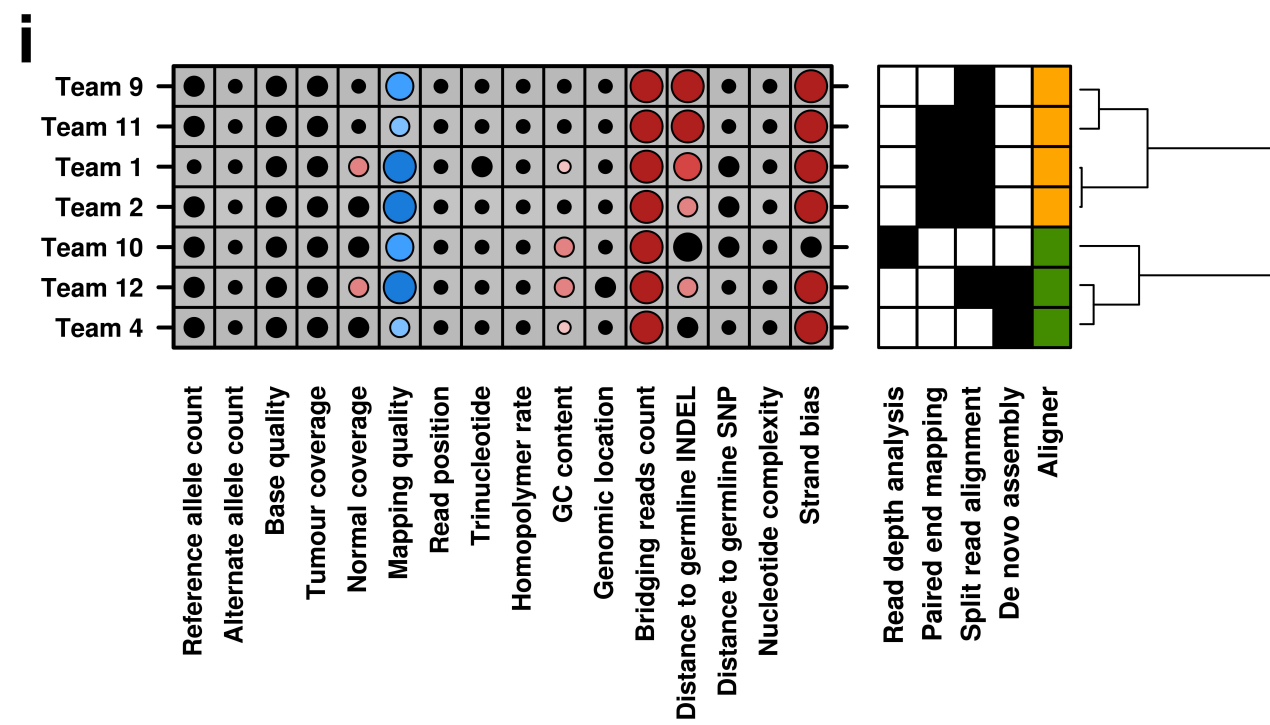
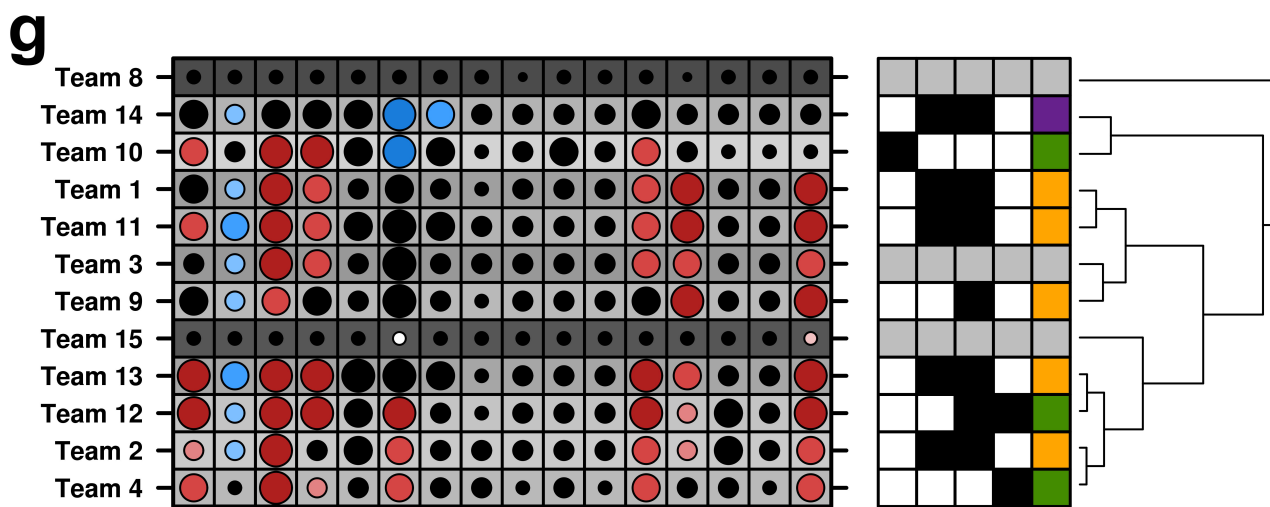
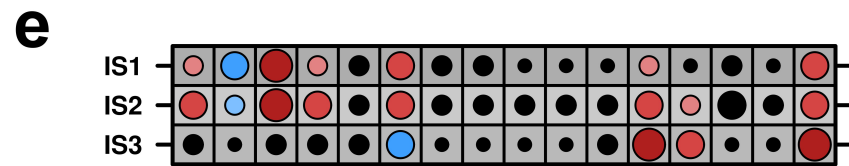
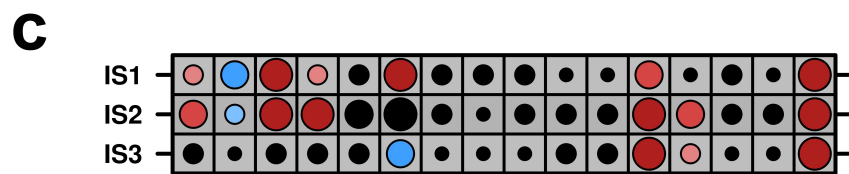
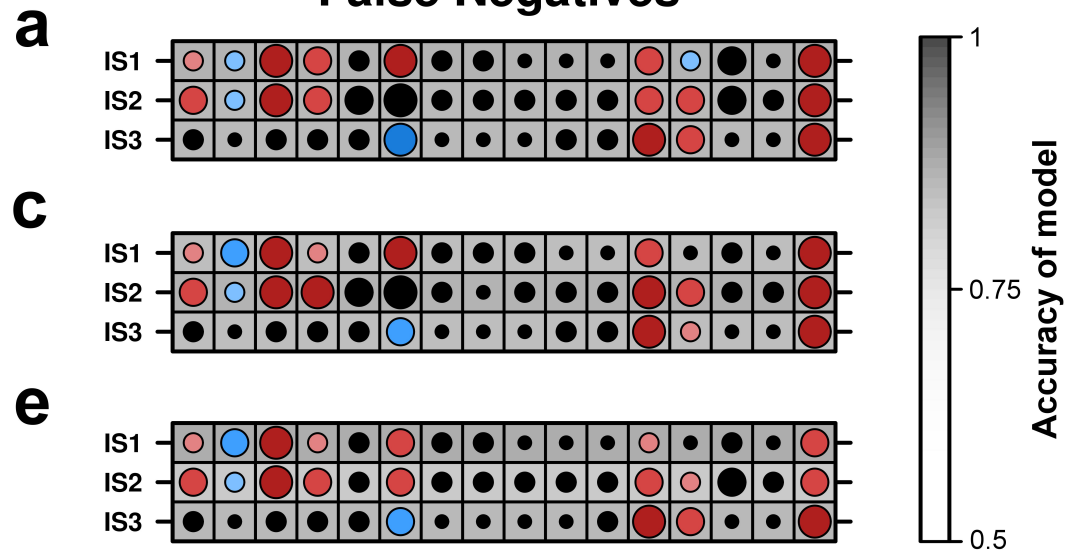
d

Tumour	Cell line	Number of somatic SVs	SV types	Cellularity (%)
<i>in silico</i> 1	HCC1143 BL	371	DEL, DUP, INV	100
<i>in silico</i> 2	HCC1954 BL	655	DEL, DUP, INV, INS	80
<i>in silico</i> 3	HCC1143 BL	2,886	DEL, DUP, INV, INS	100





False Negatives



False Positives

